Dynamical topological quantum phase transitions in nonintegrable models

I. Hagymási,[1,2,3] C. Hubig,[4] Ö. Legeza,[3] and U. Schollwöck[1,2]

[1]*Department of Physics, Arnold Sommerfeld Center for Theoretical Physics (ASC), Fakultät für Physik, Ludwig-Maximilians-Universität München, D-80333 München, Germany*
[2]*Munich Center for Quantum Science and Technology (MCQST), Schellingstr. 4, D-80799 München, Germany*
[3]*Strongly Correlated Systems "Lendület" Research Group, Institute for Solid State Physics and Optics, MTA Wigner Research Centre for Physics, Budapest H-1525 P.O. Box 49, Hungary*
[4]*Max-Planck-Institut für Quantenoptik, Hans-Kopfermann-Strasse 1, 85748 Garching, Germany*

(Dated: July 2, 2019)

We consider sudden quenches across quantum phase transitions in the $S = 1$ XXZ model starting from the Haldane phase. We demonstrate that dynamical phase transitions may occur during these quenches that are identified by nonanalyticities in the rate function for the return probability. In addition, we show that the temporal behavior of the string order parameter is intimately related to the subsequent dynamical phase transitions. We furthermore find that the dynamical quantum phase transitions can be accompanied by enhanced two-site entanglement.

Introduction.— Nonequilibrium dynamics of many-body quantum systems under unitary time evolution continue to pose a challenging problem. The time evolution of a quantum system after a sudden global quench plays a distinguished role in this field since this process can be routinely carried out in experiments and it is addressable in theoretical calculations [1].

The quench process is even more interesting when it drives the system through an equilibrium phase transition. This has opened up a new area of research named dynamical quantum phase transitions (DQPTs) [2–4]. Although they are not in one-to-one correspondence with the equilibrium phase transitions, but rather a new form of critical behavior, they often emerge when the quench crosses a phase transition. Recently, direct experimental observation of DQPTs has been reported, where a transverse-field Ising model was realized with trapped ions [5, 6]. For the better understanding of DQPTs several integrable models have been considered [4, 7–11], where the time evolution can be solved exactly. It has been revealed that, like equilibrium phase transitions, DQPTs also affect other observables. For example, when the quench starts from a broken-symmetry phase, where the order can be characterized by a local order parameter, the order parameter exhibits a temporal decay with a series of times where it vanishes [4, 12]. These times usually coincide with the times where the DQPTs occur. The case is more difficult when one considers a nonintegrable model [13–18]. Namely, the obvious choice of an observable (e.g. the equilibrium order parameter) may not follow the dynamics dictated by the DQPTs and the connection between them remains elusive like in the case of a nonintegrable Ising chain [19] or Bose-Hubbard model [20]. Thus, the relation of DQPTs to observables in nonintegrable models deserves further investigation in general.

In this work we study quenches starting from the Haldane phase to regimes where the ground state has trivial topology. The Haldane phase is a paradigmatic example of a symmetry-protected topological phase, and has direct relevance in quantum operations [21, 22]. The understanding of topological phases under unitary time evolution hence is of particular interest [23]. More precisely we examine the time evolution of the string order parameter (SOP) in the $S = 1$ XXZ model. Although this model has been investigated before regarding the thermalization of string order [24, 25], we point out that its dynamics is much richer and there is a so far unrecognized connection between the dynamics of the SOP and the underlying DQPTs, which have also not been observed before. More precisely, we consider several types of quenches and demonstrate that if a DQPT occurs during the time evolution, then it is accompanied by the zero of one of the SOPs. On the other hand, if DQPTs are not present, then all the three SOPs exhibit a smooth decay without any zeros. Such a link has been reported for a *noninteracting* system [7]. Our analysis suggests that this correspondence is not only a property of exactly solvable systems, but appears to be valid on a more general level. Moreover, our findings also reveal that the dynamics of the SOP is not only influenced by the symmetry of the quench Hamiltonian [25, 26], but by the crossing of a phase boundary as well. This conclusion is supported by a quantum information analysis of the time-evolved wave function, where the DQPT manifests itself in the enhancement of the two-site entanglement.

Model and methods.— The XXZ Heisenberg model can be written as follows:

$$\mathcal{H} = \sum_{i=1}^{L-1} [J(S_i^x S_{i+1}^x + S_i^y S_{i+1}^y) + \Delta S_i^z S_{i+1}^z] + D \sum_{i=1}^{L} (S_i^z)^2, \tag{1}$$

where S_i^α denotes the appropriate spin-1 operator component. The parameters Δ and D denote the Ising and uniaxial single-ion anisotropy, respectively and we set $J = 1$ to define the energy scale. We also set $\hbar = 1$, thus, the time is measured in units of $1/J$. The ground state of this model [27] has been thoroughly investigated

in the past few decades, and its phase diagram is now well-known [28]. Besides the symmetry-protected Haldane phase, for $D/J \gg 1$ it realizes a trivial singlet phase, for $\Delta/J \gg 1$ a Néel-like ground state, while for $\Delta/J \ll -1$ a ferromagnetic ground state occurs. Between the ferromagnetic and Haldane phases, a critical XY regime turns up. Moreover, various types of phase transitions take place at the phase boundaries allowing us to examine their dynamical counterparts within the framework of a single model. In what follows we study quenches across quantum phase transitions originating from the Haldane phase. More precisely, we initialize the system in the ground-state of the Affleck-Kennedy-Lieb-Tasaki (AKLT) Hamiltonian [29, 30], $|\Psi_0\rangle$, with $\langle\Psi_0|\sum_i S_i^z|\Psi_0\rangle = 0$, then we let it evolve unitarily governed by the Hamiltonian $\mathcal{H}$, $|\Psi(t)\rangle = e^{-i\mathcal{H}t}|\Psi_0\rangle$. The time evolution [31] is carried out using the time-dependent variational principle method [32–34].

Quench results.— Because we are not close to equilibrium by any means, the steady state is not expected to exhibit the same properties as the corresponding ground state of the postquench Hamiltonian. The positions of the phase transitions should only serve as guides when to expect the emergence of dynamical criticality. DQPTs are difficult to characterize in contrast to equilibrium phase transitions due to the lack of a free energy. Nevertheless, it has been shown by several works that they manifest themselves as nonanalyticities in the rate function of the return probability [2–4, 35]. The return probability called the Loschmidt echo $\mathcal{L}(t)$ is defined as: $\mathcal{L}(t) = |\langle\Psi_0|\Psi(t)\rangle|^2$. Since $\mathcal{L}(t)$ is not well-defined in the thermodynamic limit, it is therefore convenient to introduce the rate function, $\lambda(t)$, which reads $\lambda(t) = -\frac{1}{L}\log[\mathcal{L}(t)]$. The rate function can be regarded as a dynamical analogue of the free energy density, and just like the free energy at equilibrium phase transitions, this quantity can exhibit nonanalytic behavior at critical times as well. In one-dimensional systems the nonanalyticities show up as kinks during the time evolution.

The other important quantity of interest is the string operator, which is defined as

$$\hat{\mathcal{O}}_\ell^\alpha = \hat{S}_j^\alpha \left[\prod_{n=j+1}^{j+\ell-1} e^{i\pi\hat{S}_n^\alpha}\right] \hat{S}_{j+\ell}^\alpha \quad (\alpha \in \{x, y, z\}). \qquad (2)$$

With the help of these operators, the hidden topological order within the Haldane phase can be characterized by nonlocal order parameters [36–38], that is $\mathcal{O}^\alpha = \lim_{\ell\to\infty}\left\langle\hat{\mathcal{O}}_\ell^\alpha\right\rangle \neq 0$ should hold for any α, where the expectation value is taken with respect to the ground state. In case of the AKLT state its value is exactly $\mathcal{O}^\alpha = -4/9$ [39]. In what follows we define string order in the time-evolved state similarly, namely: $\mathcal{O}^\alpha(t) = \lim_{\ell\to\infty}\langle\Psi(t)|\hat{\mathcal{O}}_\ell^\alpha|\Psi(t)\rangle$. We study quenches into the large-D phase first. The numerical results are summarized in Figs. 1 and 2. We can easily see from Fig. 1(a) and Fig. 2 that the rate function displays distinct behavior depending on the value of D. For $D = 1$, the system is quenched in the vicinity of the phase transition point between the Haldane and the large-D phase, in spite of that, it shows completely analytic, smooth be-

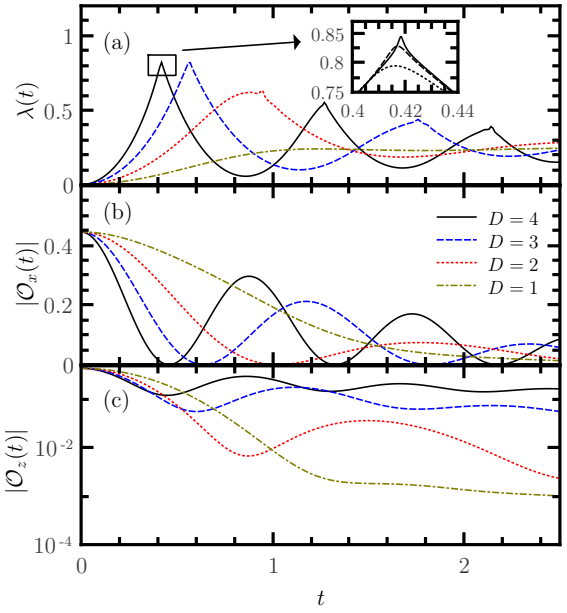

FIG. 1. (a) The main panel shows the rate function for $L = 80$, $\Delta = 1$ and various values of D as indicated by the legend in panel (b). The inset figure of panel (a) shows the finite-size effects around the first critical time for $D = 4$, the dotted, dashed and solid lines denote $L = 30, 60$ and 120, respectively. (b) The x-component of the SOP for various values of D, $\Delta = 1$ and for chain length $L = 80$. (c) The z-component of the SOP for the same parameters as in panels (a) and (b).

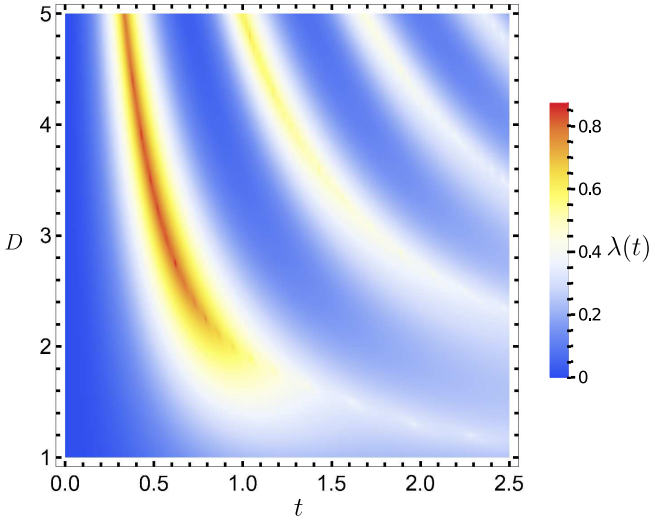

FIG. 2. The rate function as a function of time and single-ion anisotropy using a color code in the sidebar, for $\Delta = 1$ and $L = 80$.

havior. Accordingly, both $\mathcal{O}^x(t)$ and $\mathcal{O}^z(t)$ decay monotonically without any zeros. For $D = 2$, the quench drives the the system through the phase transition, and around $t \approx 1$ a tiny kink appears in the rate function. At the same time the $\mathcal{O}^x(t)$ becomes zero, while $\mathcal{O}^z(t)$ remains finite. For even larger values of D we can observe well-developed kinks in the rate functions, and they appear more frequently as the single-ion anisotropy is increased. Not only can we conclude that the difference between the positions of the kinks agree very well with the positions of the zeros of $\mathcal{O}^x(t)$, but the individual kink positions agree also well with the zeros of $\mathcal{O}^x(t)$. We can also notice that the regions where $\mathcal{O}^x(t)$ shows local maxima coincide with the local minima of the rate function. In the inset of Fig. 1(a) we can observe the finite-size dependence of the rate function around the critical times. We can indeed identify that a kink is being developed as the system size is increased, thus, for infinite system size, the time-evolved state becomes completely orthogonal to the initial state inducing a DQPT in the system. At these critical times, the system should possess trivial topology, since $\mathcal{O}^x(t)$ vanishes here. It is also worth mentioning that $\mathcal{O}^z(t)$ decays smoothly with some superimposed oscillations for larger D, but it does not show any zeros in this time window. Interestingly, it decays slower in time for larger values of D. This seems to be analogous to what happens during an interaction quench in the Fermi-Hubbard model. Namely, when the quench drives the system from a weakly interacting regime to a strongly interacting one, then the relaxation time of the double occupancy increases exponentially with the Hubbard-U [40, 41]. In our case, the nonzero spin components play the same role, when we quench to the large-D phase.

Next, we turn our attention to quenches into the Néel regime. In that case already for $\Delta = 2$ well-developed kinks are observable. Similarly, the zeros of the $\mathcal{O}^x(t)$ are in excellent agreement with the kinks in the rate function. In addition, $\mathcal{O}^z(t)$ remains always nonzero, moreover, its value is slightly increased after the quench. This may not surprise us, if we recall that the Ising term with $\Delta > 1$ enhances the antiferromagnetic correlations leading therefore to an increased string correlation value in the z direction.

We also consider quenches with $\Delta < 0$ [31], which corresponds to probing the spectrum of the XY and the ferromagnetic phase. In these cases we find no signs of DQPTs in the rate function and the SOP decays without any zeros in time. It is worth noting that the relation between the DQPTs and the SOP holds even if the model has fewer symmetries [31] or in the full SU(2)-symmetric bilinear-biquadratic chain for the Haldane–dimerized transition.

Discussion.— Having seen how the rate function and the SOPs behave in the different cases, the question naturally arises if we can say something more to account for the different behavior in the $\Delta < 0$ cases. Our only guide

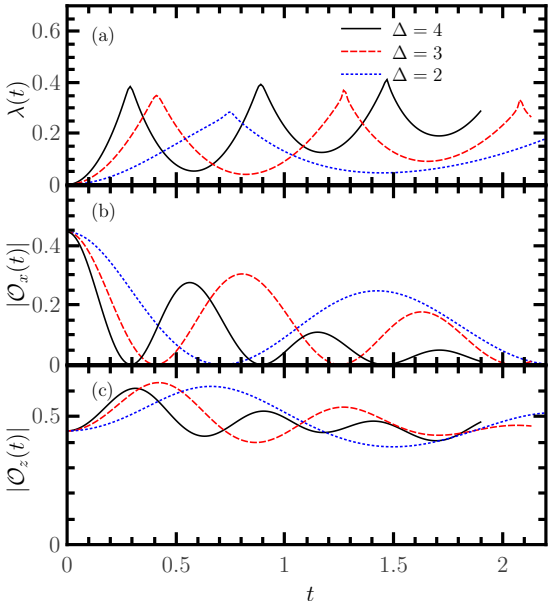

FIG. 3. (a) The rate function for various values of Δ and $D = 0$. Panels (b) and (c) show the x- and z-component of the SOP for the same values of Δ and $D = 0$ as in panel (a). The chain length is $L = 80$ in all cases.

is the phase diagram [28]. When we quench to the Néel or the large-D phase, we face in both cases a second-order phase transition. More precisely, the Haldane–large-D critical line is a Gaussian-, while the Haldane–Néel one is an Ising-type phase transition [28]. During these quenches we cross the critical lines, where the spectrum is expected to be gapless. Thus, this drastic change manifests itself in the appearance of DQPTs in both cases. In contrast, when we quench to the XY phase, an infinite-order phase transition takes place at the phase boundary [28]. Since the gap opens here exponentially slowly, it may prevent the occurrence of DQPTs. During the quench from the Haldane phase to the ferromagnetic phase, two phase transitions are encountered, infinite order (Haldane to XY) and first order (XY to ferromagnetic) [28]. The lack of DQPTs in this case can be traced back to several reasons. A first-order transition involves a level crossing of the ground state with a higher-lying state at the transition point, but the whole spectrum does not change so drastically at the transition point like in the case of a second-order transition. Another reason, which could also apply for the quench in the XY regime, is that DQPTs may occur at a later time and simply our simulation time is not long enough.

Quantum information analysis.— In the analysis of equilibrium quantum phase transitions the tools of the quantum information theory turned out to be extremely useful [42–47]. The entropies of various subsystems can be sensitive indicators for phase transitions but also for characterizing the entanglement structure of the wave function [48–51], especially through the mutual infor-

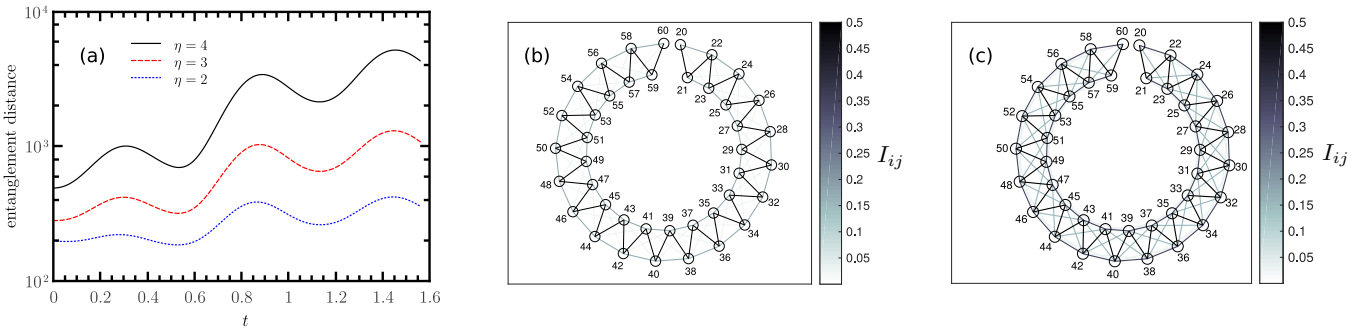

FIG. 4. (a) The entanglement distance as a function of time calculated with different exponents for the quench with $\Delta = 4$, $D = 0$. (b) The entanglement patterns in the chain at time $t = 0.53$ for the same quench as in panel (a). The lines encode the magnitude of the mutual information between different sites using the grayscale sidebar. Note that 20 sites are discarded at both ends. (c) Similar to panel (b) but for $t = 0.89$. The chain length is $L = 80$ in all cases.

mation, I_{ij}, defined as $I_{ij} = s_i + s_j - s_{ij}$, which measures all correlations both of classical and quantum origin between sites i and j. Here s_i and s_{ij} denote the one- and two-site entropies of the corresponding sites. One can naturally ask if there appear some anomalous signatures in these quantities around the critical times. The entanglement entropy in global quenches, like ours, increases linearly with the time, thus complicating the analysis. It has been reported before that the DQPTs may result in enhanced entropy production around the critical times [5]. We ask the question if DQPTs affect the two-site entanglement, since it is easier to interpret than the whole entanglement entropy, which contains the cumulated effects of several physical processes. To this end, we adopt the entanglement distance [52, 53], $I^{(\eta)}_{\rm dist}$, to quantify the strength of the two-site entanglement in the system: $I^{(\eta)}_{\rm dist} = \sum_{ij} I_{ij}|i-j|^{\eta}$. Different η exponents have been used in the literature. For negative (positive) values of η it emphasizes the contribution of short-range (long-range) entanglement [52, 53]. We calculate this quantity using different exponents to study the delocalization of the entanglement during the time evolution. This is shown in Fig. 4(a) in the case when the quench goes through the Haldane–Néel transition line. Remarkably, $I^{(\eta)}_{\rm dist}$ does not increase monotonically as one would naively expect from the linear increase of the entanglement entropy (not shown). More surprising is the fact that the positions of the maxima in $I^{(\eta)}_{\rm dist}$ agree very well with the positions of the DQPTs. We can interpret this phenomenon such that the two-site correlations get enhanced around the critical times, resembling to the long-range correlations occurring at the equilibrium phase transition. It is important to note, however, that truly long-range correlations cannot occur in our case, since the Lieb-Robinson bound does not allow the instantaneous buildup of long-ranged correlations [54, 55]. We illustrate this enhancement in Fig. 4(b) and (c), where the two times correspond to a local minimum and maximum in $I^{(\eta)}_{\rm dist}$, respectively.

We also checked if a similar connection exists for the quench through the Haldane–large-D line. Although we found that $I^{(\eta)}_{\rm dist}$ is also a nonmonotonic function of time, its relation to the DQPTs is less clear. This discrepancy may be understood with the help of the following argument: the quantum critical point, in a strict sense, shows up only at zero temperature, the critical fluctuations, however, influence the finite-temperature properties as well, which can be detected in a wide range of temperatures. In our case, the quench energy can be regarded as an effective temperature, and by crossing a a quantum critical point, we probe the critical region 'above' the critical point. Since the universality classes of the two phase transitions are distinct, the associated critical regions are also expected to display different behavior.

Conclusions.— We examined the nonequilibrium dynamics of the Haldane phase under unitary time evolution in the XXZ model. We revealed that DQPTs can occur when the quench crosses a phase boundary and they manifest themselves in nonanalyticities in the rate function for the Loschmidt echo. Moreover, we demonstrated that there is an intrinsic connection between the nonanalyticities and the zeros of the SOP. Thus, the emerging nonequilibrium time scale has also fingerprints in other observable quantities. Using the tools of quantum information theory we pointed out that the two-site entanglement may get significantly enhanced in the vicinity of the DQPTs exhibiting some resemblance to equilibrium phase transitions. Since both the Loschmidt echo and SOP are now within the reach of experimental techniques [5, 56], our findings could be also directly tested in the future. In recent experiments effective spin-1 chains have already been successfully simulated with trapped ions [57].

Acknowledgments.—We acknowledge discussions with N. Cooper and M. McGinley. I.H. and Ö.L. were supported by the Alexander von Humboldt Foundation and in part by Hungarian National Research, Devel-

opment and Innovation Office (NKFIH) through Grant No. K120569 and the Hungarian Quantum Technology National Excellence Program (Project No. 2017-1.2.1-NKP-2017-00001). C.H. acknowledges funding through ERC Grant QUENOCOBA, ERC-2016-ADG (Grant no. 742102). This work was also supported in part by the Deutsche Forschungsgemeinschaft (DFG, German Research Foundation) under Germanys Excellence Strategy – EXC-2111 – 390814868.

[1] F. H. L. Essler and M. Fagotti, J. Stat. Mech.: Theory and Exp. **2016**, 064002 (2016).
[2] M. Heyl, Phys. Rev. Lett. **115**, 140602 (2015).
[3] M. Heyl, Rep. Prog. Phys. **81**, 054001 (2018).
[4] M. Heyl, A. Polkovnikov, and S. Kehrein, Phys. Rev. Lett. **110**, 135704 (2013).
[5] P. Jurcevic, H. Shen, P. Hauke, C. Maier, T. Brydges, C. Hempel, B. P. Lanyon, M. Heyl, R. Blatt, and C. F. Roos, Phys. Rev. Lett. **119**, 080501 (2017).
[6] N. Fläschner, D. Vogel, M. Tarnowski, B. S. Rem, D. S. Lühmann, M. Heyl, J. C. Budich, L. Mathey, K. Sengstock, and C. Weitenberg, Nat. Phys. **14**, 265 (2018).
[7] J. C. Budich and M. Heyl, Phys. Rev. B **93**, 085416 (2016).
[8] S. Vajna and B. Dóra, Phys. Rev. B **91**, 155127 (2015).
[9] S. Vajna and B. Dóra, Phys. Rev. B **89**, 161105(R) (2014).
[10] J. Lang, B. Frank, and J. C. Halimeh, Phys. Rev. B **97**, 174401 (2018).
[11] J. Lang, B. Frank, and J. C. Halimeh, Phys. Rev. Lett. **121**, 130603 (2018).
[12] S. A. Weidinger, M. Heyl, A. Silva, and M. Knap, Phys. Rev. B **96**, 134313 (2017).
[13] J. C. Halimeh and V. Zauner-Stauber, Phys. Rev. B **96**, 134427 (2017).
[14] V. Zauner-Stauber and J. C. Halimeh, Phys. Rev. E **96**, 062118 (2017).
[15] I. Homrighausen, N. O. Abeling, V. Zauner-Stauber, and J. C. Halimeh, Phys. Rev. B **96**, 104436 (2017).
[16] T. Hashizume, I. P. McCulloch, and J. C. Halimeh, arXiv:1811.09275.
[17] J. C. Halimeh, M. V. Damme, V. Zauner-Stauber, and L. Vanderstraeten, arXiv:1810.07187 ().
[18] J. C. Halimeh, N. Yegovtsev, and V. Gurarie, arXiv:1903.03109 ().
[19] C. Karrasch and D. Schuricht, Phys. Rev. B **87**, 195104 (2013).
[20] T. Fogarty, A. Usui, T. Busch, A. Silva, and J. Goold, New J. Phys. **19**, 113018 (2017).
[21] A. S. Darmawan and S. D. Bartlett, Phys. Rev. A **82**, 012328 (2010).
[22] D. V. Else, I. Schwarz, S. D. Bartlett, and A. C. Doherty, Phys. Rev. Lett. **108**, 240505 (2012).
[23] M. McGinley and N. R. Cooper, Phys. Rev. B **99**, 075148 (2019).
[24] M. Calvanese Strinati, L. Mazza, M. Endres, D. Rossini, and R. Fazio, Phys. Rev. B **94**, 024302 (2016).
[25] L. Mazza, D. Rossini, M. Endres, and R. Fazio, Phys. Rev. B **90**, 020301(R) (2014).
[26] M. McGinley and N. R. Cooper, Phys. Rev. Lett. **121**, 090401 (2018).
[27] R. Botet, R. Jullien, and M. Kolb, Phys. Rev. B **28**, 3914 (1983).
[28] W. Chen, K. Hida, and B. C. Sanctuary, Phys. Rev. B **67**, 104401 (2003).
[29] I. Affleck, T. Kennedy, E. H. Lieb, and H. Tasaki, Phys. Rev. Lett. **59**, 799 (1987).
[30] This special choice for the initial state does not restrict the validity of our calculations, since it belongs evidently to the Haldane phase and has simple matrix-product-state representation with bond dimension $M = 2$, on the other hand it enables us to reach longer times, with high accuracy. Simulations with the ground state corresponding to $D = 0$ and $\Delta = 1$ does not give qualitatively different results.
[31] See Supplemental Material at [URL will be inserted by publisher] for more numerical details and for the quench results with $\Delta < 0$, which includes Refs. [3, 32–34, and 58].
[32] J. Haegeman, J. I. Cirac, T. J. Osborne, I. Pižorn, H. Verschelde, and F. Verstraete, Phys. Rev. Lett. **107**, 070601 (2011).
[33] J. Haegeman, C. Lubich, I. Oseledets, B. Vandereycken, and F. Verstraete, Phys. Rev. B **94**, 165116 (2016).
[34] S. Paeckel, T. Köhler, A. Swoboda, S. R. Manmana, U. Schollwöck, and C. Hubig, arXiv:1901.05824.
[35] L. Piroli, B. Pozsgay, and E. Vernier, Nucl. Phys. B **933**, 454 (2018).
[36] M. den Nijs and K. Rommelse, Phys. Rev. B **40**, 4709 (1989).
[37] F. Pollmann, A. M. Turner, E. Berg, and M. Oshikawa, Phys. Rev. B **81**, 064439 (2010).
[38] F. Pollmann and A. M. Turner, Phys. Rev. B **86**, 125441 (2012).
[39] A. Klümper, A. Schadschneider, and J. Zittartz, Europhys. Lett. (EPL) **24**, 293 (1993).
[40] M. Eckstein and P. Werner, Phys. Rev. B **84**, 035122 (2011).
[41] P. Werner, N. Tsuji, and M. Eckstein, Phys. Rev. B **86**, 205101 (2012).
[42] Ö. Legeza and J. Sólyom, Phys. Rev. B **68**, 195116 (2003).
[43] G. Vidal, J. I. Latorre, E. Rico, and A. Kitaev, Phys. Rev. Lett. **90**, 227902 (2003).
[44] P. Calabrese and J. Cardy, J. Stat. Mech. **2004**, P06002 (2004).
[45] J. Rissler, R. M. Noack, and S. R. White, Chem. Phys. **323**, 519 (2006).
[46] Ö. Legeza and J. Sólyom, Phys. Rev. Lett. **96**, 116401 (2006).
[47] L. Amico, R. Fazio, A. Osterloh, and V. Vedral, Rev. Mod. Phys. **80**, 517 (2008).
[48] S.-J. Gu, S.-S. Deng, Y.-Q. Li, and H.-Q. Lin, Phys. Rev. Lett. **93**, 086402 (2004).
[49] L.-A. Wu, M. S. Sarandy, and D. A. Lidar, Phys. Rev. Lett. **93**, 250404 (2004).
[50] M.-F. Yang, Phys. Rev. A **71**, 030302(R) (2005).
[51] S.-S. Deng, S.-J. Gu, and H.-Q. Lin, Phys. Rev. B **74**, 045103 (2006).
[52] G. Barcza, Ö. Legeza, K. H. Marti, and M. Reiher, Phys. Rev. A **83**, 012508 (2011).
[53] J. Rissler, R. M. Noack, and S. R. White, Chemical

Physics **323**, 519 (2006).
[54] T. D. Schultz, D. C. Mattis, and E. H. Lieb, Rev. Mod. Phys. **36**, 856 (1964).
[55] E. H. Lieb and D. W. Robinson, Commun. Math. Phys. **28**, 251 (1972).
[56] T. A. Hilker, G. Salomon, F. Grusdt, A. Omran, M. Boll, E. Demler, I. Bloch, and C. Gross, Science **357**, 484 (2017).
[57] C. Senko, P. Richerme, J. Smith, A. Lee, I. Cohen, A. Retzker, and C. Monroe, Phys. Rev. X **5**, 021026 (2015).
[58] G. D. Chiara, S. Montangero, P. Calabrese, and R. Fazio, J. Stat. Mech.: Theory and Exp. **2006**, P03001 (2006).